

ORIGINAL RESEARCH

Breast Cancer Promotes Cardiac Dysfunction Through Deregulation of Cardiomyocyte Ca²⁺-Handling Protein Expression That is Not Reversed by Exercise Training

Tassia S. R. da Costa , PhD; Ursula Urias , PhD; Marcelo V. Negrao , MD; Camila P. Jordão , MS; Clévia S. Passos , PhD; Igor L. Gomes-Santos , PhD; Vera Maria C. Salemi , MD, PhD; Anamaria A. Camargo , PhD; Patricia C. Brum , PhD; Edilamar M. Oliveira , PhD; Ludhmila A. Hajjar , MD, PhD; Roger Chammas , MD, PhD; Roberto K. Filho, MD, PhD; Carlos E. Negrao , PhD

BACKGROUND: Patients treated for breast cancer have a high incidence of cardiovascular complications. In this study, we evaluated the impact of breast cancer on cardiac function and cardiomyocyte Ca²⁺-handling protein expression. We also investigated whether exercise training (ET) would prevent these potential alterations.

METHODS AND RESULTS: Transgenic mice with spontaneous breast cancer (mouse mammary tumor virus–polyomavirus middle T antigen [MMTV-PyMT+], n=15) and littermate mice with no cancer (MMTV-PyMT–, n=14) were studied. For the ET analysis, MMTV-PyMT+ were divided into sedentary (n=10) and exercise-trained (n=12) groups. Cardiac function was evaluated by echocardiography with speckle-tracking imaging. Exercise tolerance test was conducted on a treadmill. Both studies were performed when the tumor became palpable and when it reached 1 cm³. After euthanasia, Ca²⁺-handling protein expression (Western blot) was evaluated. Exercise capacity was reduced in MMTV-PyMT+ compared with MMTV-PyMT– ($P_{\text{interaction}}=0.031$). Longitudinal strain ($P_{\text{group}} < 0.001$) and strain rate ($P_{\text{group}}=0.030$) were impaired. Cardiomyocyte phospholamban was increased ($P=0.011$), whereas phospho-phospholamban and sodium/calcium exchanger were decreased ($P=0.038$ and $P=0.017$, respectively) in MMTV-PyMT+. No significant difference in sarcoplasmic or endoplasmic reticulum calcium 2 ATPase (SERCA2a) was found. SERCA2a/phospholamban ratio was reduced ($P=0.007$). ET was not associated with increased exercise capacity. ET decreased left ventricular end-systolic diameter ($P_{\text{group}}=0.038$) and end-diastolic volume ($P_{\text{group}}=0.026$). Other morphological and functional cardiac parameters were not improved by ET in MMTV-PyMT+. ET did not improve cardiomyocyte Ca²⁺-handling protein expression.

CONCLUSIONS: Breast cancer is associated with decreased exercise capacity and subclinical left ventricular dysfunction in MMTV-PyMT+, which is at least partly associated with dysregulation of cardiomyocyte Ca²⁺ handling. ET did not prevent or reverse these changes.

Key Words: breast cancer ■ Ca²⁺ handling ■ cardiac function

Breast cancer is the most diagnosed cancer among women, and it was responsible for more than 2 million new cancer cases worldwide in

2018.¹ Multimodality treatment, which includes surgical resection, radiation, and systemic therapy, is the current standard of care for this disease.²

Correspondence to: Carlos E. Negrao, PhD, Heart Institute (InCor), University of Sao Paulo Medical School, Av. Dr. Enéas de Carvalho Aguiar, 44 – Cerqueira César – São Paulo, SP CEP 05403-904 Brazil. E-mail: cndnegrao@incor.usp.br

Supplementary Material for this article is available at <https://www.ahajournals.org/doi/suppl/10.1161/JAHA.120.018076>

For Sources of Funding and Disclosures, see page 11.

© 2021 The Authors. Published on behalf of the American Heart Association, Inc., by Wiley. This is an open access article under the terms of the Creative Commons Attribution-NonCommercial-NoDerivs License, which permits use and distribution in any medium, provided the original work is properly cited, the use is non-commercial and no modifications or adaptations are made.

JAHA is available at: www.ahajournals.org/journal/jaha

CLINICAL PERSPECTIVE

What Is New?

- Breast cancer is associated with subclinical left ventricular dysfunction in transgenic mice with spontaneous breast cancer at the end stage of this disease.
- This cardiac dysfunction is associated with dysregulation of cardiomyocyte Ca²⁺ handling.
- Exercise training alone is not an effective strategy to prevent or reverse the cardiac function provoked by breast cancer.

What Are the Clinical Implications?

- These findings highlight that cancer is a systemic disease that gradually compromises body homeostasis as the disease progresses.
- Moreover, it is suggested that patients with cancer are more susceptible to organ dysfunction, including cardiac dysfunction.

Nonstandard Abbreviations and Acronyms

EjT	ejection time
ERK	extracellular signal-regulated kinase
ET	exercise training
ETT	exercise tolerance test
HER2	human epidermal growth factor receptor type 2
IVCT	isovolumetric contraction time
IVRT	isovolumetric relaxation time
IVS	interventricular septum
JNK	c-Jun N-terminal kinase
LVEDD	left ventricular end-diastolic diameter
LVESD	left ventricular end-systolic diameter
LVESV	left ventricular end-systolic volume
LVPW	posterior wall thickness
MAPK	mitogen-activated protein kinase
MMTV	mouse mammary tumor virus
PI3K	phosphoinositide 3-kinase
p-Phospholamban	phospho-phospholamban
PyMT	polyomavirus middle T antigen
SERCA2a	sarcoplasmic or endoplasmic reticulum calcium 2 ATPase

Systemic agents commonly used to treat breast cancer, such as anthracyclines, are known to be associated with cardiovascular events, a phenomenon known as cardiovascular toxicity.³ Endothelial dysfunction,⁴ acute coronary syndrome,⁵ supraventricular and ventricular arrhythmias,⁶ and ventricular dysfunction,⁷ leading to heart failure,⁸ have all been described in patients during or after chemotherapy treatment. However, little is known about the impact of breast cancer itself on cardiac function, which can be important to clarify the impact of cancer as a systemic disease that can negatively affect the cardiovascular physiology.

Exercise training (ET) promotes many benefits to the cardiovascular system both in healthy and chronically ill individuals. Previous studies from our group demonstrated that ET improves cardiac function in hypercaloric obese rats and in a mouse model of heart failure induced by sympathetic hyperactivity.^{9,10} In addition, ET substantially increases physical capacity^{9,10} and is considered a marker of ET adaptation.

In this study, we hypothesized that breast cancer would promote cardiac dysfunction and decrease exercise tolerance. We also hypothesized that ET would attenuate or prevent cancer-induced cardiac dysfunction. To understand the effects of breast cancer on cardiac function, we used a mouse model of breast cancer. We used this same model to explore the effects of ET on cardiac function, and to test whether the changes in cardiac function were associated with deregulation of Ca²⁺ handling in the mouse cardiomyocyte.

METHODS

The data, analytical methods, and study materials that support the conclusions of this study will be available to other researchers for the purpose of replicating the procedures and reproducing the results through reasonable request by contacting the corresponding author.

Animal Model

Female mice carrying the polyomavirus middle T antigen (mouse mammary tumor virus [MMTV]-PyMT+), a transgenic mouse model of spontaneous breast cancer with C57BL6/J genetic background, from University of São Paulo Medical School, were used in the study, and their respective healthy offspring (MMTV-PyMT-) served as controls. In these mice, the development of spontaneous breast cancer in 4 distinctly identifiable stages of tumor progression occurs in a single primary tumor focus and it resembles the pathology of human breast cancer in relation to hyperplasia, adenoma, and early and late carcinoma.¹¹⁻¹³ In addition, the loss of estrogen and progesterone receptors and the overexpression of

human epidermal growth factor receptor type 2 (HER2) are similar to HER2-amplified human breast cancer.

Mice were kept in the animal facilities of the University of São Paulo Medical School, placed in a standard mouse polypropylene box (30×20×13 cm) with a meshed lid and lined with sterile wood shavings. The animals were housed 4 per cage and kept at controlled temperatures of 22 to 24°C, with relative humidity of 45% to 50%, and reversed light-dark cycle in 12-hour day and night periods. Meals included standard mice chow and water ad libitum. All animal procedures were approved by the Scientific Committee for Animal Research from the University of São Paulo Medical School (N°061/16). The experiment was conducted in concordance with the National Council for Animal Experimentation Control.

Experimental Protocol

In a pilot study to test the hypothesis regarding cardiac function analysis, the sample size (n=4 per group) was reconsidered because of the variability in the results. In addition, some histological and molecular techniques widely used in previous studies highlight a minimum number of 5 animals for tissue biodistribution.¹⁴ The sample size calculation based on the longitudinal strain of the first 5 animals of each group from the substudy 1 (pilot) showed the average value of -10.3% with 1.9% (SD) variability in the group with cancer (MMTV-PyMT+) after the period of tumor development and the average value of -12.9% with 2.6% (SD) variability in the group without cancer (MMTV-PyMT-) after the corresponding period of the experimental protocol. Expecting that these differences would be maintained in the total sampling with a power of 80% and confidence of 95% (α of 5%), the sample size would be 13 animals in each group. Thus, 14 and 15 mice were included in the substudy 1. In the complementary study (substudy 2), 10 to 12 mice were involved in the experiment. All animals were monitored by high-resolution echocardiographic imaging and exercise tolerance test (ETT), with the exception of 1 animal in the sedentary group, which died during the experimental protocol.

The mice were matched for age under the same environmental conditions. This experiment began when the tumor became palpable, which occurred around the 12th week of age and 20 g body weight and ended when the tumor reached 1 cm³ (average: 22 weeks), according to regulations from the Scientific Committee for Animal Research of the University of São Paulo Medical School. Body weight was assessed every week and tumor growth every 2 to 3 days.¹⁵ Echocardiography and ETT were conducted at the beginning and at the end of the experiment. When tumors reached 1 cm³, the animals were

ethanized after lethal dose by isoflurane (5%) inhalation. After loss of consciousness and motor activity, there was exsanguination and removal of tissues for analysis. Lungs, liver, spleen, kidneys, white and brown fat, anterior tibial and soleus muscles, and tumors were weighed and banked (Figure 1). The heart was only deposited.

Next, we randomized MMTV-PyMT+ mice into 2 groups: sedentary (n=10) and exercise-trained (n=12). The animals were matched for age and selected in a systematic random manner. ECG and ETT evaluation were performed when the tumor became apparent and when it reached 1 cm³. In addition, the ETT was performed every 4 weeks during the experimental protocol to readjust training intensity. The test was performed in the control group in the same period. Body weight was assessed every week and tumor growth every 2 to 3 days.¹⁵ At the end of the protocol, all animals were euthanized after lethal dose by isoflurane (5%) inhalation. After loss of consciousness and motor activity, there was exsanguination and removal of tissues for analysis. Heart, liver, spleen, kidneys, white and brown fat, anterior tibial and soleus muscles, and tumors were weighed and banked for analysis (Figure 1). The lungs were only inflated and stored for further analysis.

The researchers analyzing the study samples were blinded to the experimental arms to assure both animal experiments were performed in a blinded manner.

Measures and Procedures

During the experimental protocol, measurements were performed in the morning, while the functional procedures were performed in the afternoon.

Exercise Tolerance Test

ETT was performed on a motor treadmill as previously described.¹⁶ In brief, exercise started with a

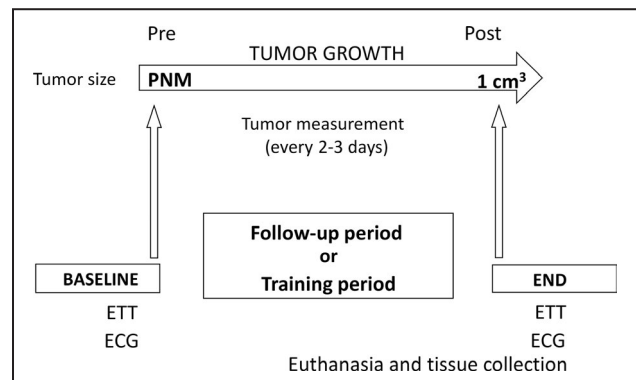


Figure 1. Experimental protocol.

ETT indicates exercise tolerance test; PNM, palpable and not measurable tumor; Pre, pre phase tumor growth (BASELINE); and Post, post phase tumor growth (END).

6-m/min speed increment of 3 m/min every 3 minutes up to the maximal speed tolerated. Exhaustion was determined when the mice could no longer run despite further speed increment. The maximal distance, maximal velocity, and duration of the exercise were registered.

ET Protocol

ET was performed on a treadmill at 50% to 60% of the maximal speed achieved in the ETT. Training sessions occurred 5 times a week,¹⁶ with a session duration of 60 minutes.

High-Resolution Echocardiography

To assess cardiac morphology and function, transthoracic high-resolution echocardiography was performed using a Vevo 2100 system (Visual Sonics) with an MS400 (30-MHz centerline frequency) probe. In brief, mice were anesthetized with isoflurane (Zoetis IsoFlo; induction 3.0% and maintenance 1%–3%) and hair was removed from the chest. Mice were subsequently placed in the supine position on a heated table with embedded ECG leads and the core temperature maintained at 37°C. Anesthesia was maintained with 1% to 3% isoflurane throughout the study. Image acquisition was performed by 2-dimensional mode in the parasternal long-axis view followed by the short-axis and apical 4-chamber views. Two-dimensional guided M-mode imaging was used to measure left ventricular (LV) end-diastolic diameter (LVEDD), LV end-systolic diameter (LVESD), interventricular septum (IVS), and posterior wall thickness (LVPW), corrected by body weight. Also, the LV end-diastolic volume (LVEDV), LV end-systolic volume (LVESV) and mass (Left ventricular mass = $0.8 \times \{1.04 \times [(LVEDD + LVPW + IVS)^3 - (LVEDD)^3]\}$), both corrected by body weight, fractional shortening (Fractional shortening = $[(LVEDD - LVESD) / LVEDD] \times 100$), and ejection fraction by Teichholz method were calculated from M-mode echocardiography.¹⁷ Left atrium (LA) diameter was acquired from 2-dimensional parasternal long-axis view. Diastolic function was evaluated using conventional echocardiography with tissue Doppler imaging and pulsed-wave Doppler techniques. Transmitral inflow velocities were recorded from an apical long-axis view by setting the sample volume in the tip of the mitral leaflets. From the pulsed-wave Doppler spectral waveforms, the peak early- and late-diastolic transmitral velocities (E and A waves) to obtain the E/A ratio were measured. E-wave deceleration time and isovolumetric relaxation time (IVRT) were corrected by heart rate dividing them by the square root of the R-R interval. Isovolumetric contraction time (IVCT) and ejection time (EJT) were measured

to obtain myocardium performance index (Myocardium performance index = $(IVCT + IVRT) / EJT$). From the tissue Doppler spectral waveforms, E' (early diastolic mitral annular peak velocity at the septum) was measured and E/E' ratio was calculated.¹⁷

Speckle-tracking imaging analyses were performed on parasternal long-axis and short-axis view (papillary level) using a Visual Sonics Vevo 2100 system (Visual Sonics). Image depth, width, and gain settings were optimized to improve image quality. Two-dimensional loops with a frame rate ≥ 200 frame/s were utilized for speckle-tracking imaging. All images were digitally stored in cine loops consisting of 300 frames, acquired, and then analyzed using Vevo Strain Software (Vevo LAB1.7.1). Strain, which evaluates length changes relative to initial length, was calculated either in the radial short- and long-axis (thickening of the LV wall along radius axis) or longitudinally (shortening of the LV wall along long axis) and circumferentially (reduction in the circumference of the LV cavity). Strain rate, defined as the rate of change of this deformation over time, was also measured.¹⁸

Cardiac Morphological and Structural Analysis

Heart sections were fixed in 10% buffered formalin for 48 hours. After routine histologic processing, paraffin-embedded tissue was sectioned (5- μ m-thick sections) and the histologic slides were stained with hematoxylin-eosin and Sirius red for quantitative analysis of cardiomyocyte diameters and of collagen rate, respectively. Measurement of the transverse diameter of the cardiomyocytes was performed in a computerized system (LEICA QUANTIMET 500) coupled with a $\times 40$ magnification optical microscope. Cardiomyocyte diameter was calculated from an average of all fields of a single cut of the LV per animal, considering the fibers intact. The degree of myocardial fibrosis was analyzed by means of a complete ventricular wall scan performed under a polarized light optical microscope (OLYMPUS BX-41) at $\times 40$ magnification. The type I collagen (yellowish orange and reddish orange) and type III collagen (green or yellowish green) were evaluated by staining. The analysis was performed by ImageJ software (National Institutes of Health) using the threshold color plug-in to obtain the collagen percentage by analyzing the stained pixels according to the area measurement. Threshold color values for each collagen type were standardized: matrix 0 to 40 for collagen type I red color and 45 to 120 for collagen type III green color, with saturation 0 to 255 and brightness 5 to 225 for both.

Expression of Protein Levels Analysis by Western Blot

The protein levels of sodium/calcium exchanger, sarcoplasmic or endoplasmic reticulum calcium ATPase

cardiac isoform 2a (SERCA2a), and phospholamban and phospho-phospholamban (p-phospholamban) in the heart muscle lysate were analyzed by Western blot. Frozen samples were homogenized in cell lysis buffer (100 mmol/L TrisHCl, 50 mmol/L NaCl, 1% Triton X-100) and protease and phosphatase inhibitor cocktail (1:100; Sigma-Aldrich). Heart tissue debris was removed by centrifugation at 3000g, 4°C, for 10 minutes. Samples were loaded and subjected to SDS-PAGE on polyacrylamide gels (8%–15%) depending on the protein molecular weight. After electrophoresis, proteins were electrotransferred to a nitrocellulose membrane (BioRad Biosciences). Equal loading of samples (30 µg) and even transfer efficiency were monitored with the use of 0.5% Ponceau staining of the blot membrane. The blot membrane was then incubated in a blocking buffer (5% bovine serum albumin, 10 mmol/L Tris-HCl [pH 7.6], 150 mmol/L NaCl, and 0.1% Tween 20) for 2 hours at room temperature and then incubated overnight at 4°C with anti-sodium/calcium exchanger (Thermo Fisher, #MA3-926), anti-SERCA2 ATPase (Thermo Fisher, #MA3-919), anti-phospholamban (Thermo Fisher, #MA3-922), and anti-p-phospholamban^{Ser16,Thr17} (Thermo Fisher, #711401) antibodies. Binding of the primary anti-sodium/calcium exchanger, anti-SERCA2 ATPase, anti-phospholamban, anti-p-phospholamban^{Ser16,Thr17}, and anti-GAPDH was detected by secondary antibody (IRDye 800CW anti-mouse [#926-32210] or IRDye 800CW anti-rabbit [#926-32211], and LI-COR Biosciences), and detection was performed by LI-COR (LI-COR Biosciences). The bands were analyzed using Image Studio Lite software (LI-COR Biosciences). The results of protein expression were normalized by Ponceau staining. They are expressed as a percentage of control expression for each group. Of note, the Western blot assays were run in triplicate for all of the Ca²⁺-handling proteins, with the exception of the p-phospholamban protein, performed in duplicate.

Citrate Synthase Activity

Activity of citrate synthase enzyme in the anterior tibial and soleus muscles was evaluated as a marker of ET effectiveness. The enzyme activity was determined by means of commercial citrate synthase assay kit (Sigma-Aldrich).

Statistical Analysis

Values are expressed as means±SD or medians and interquartile range (IQR). Animal body weights were evaluated weekly, but only the values of every 2 weeks were used for the analysis. The echocardiogram and speckle tracking measures were compared according to group and time of evaluation using generalized estimation equations with normal marginal distribution

and identity link function, assuming a first-order autoregressive correlation matrix between moments.¹⁹ In case of significant difference, the results were followed by Bonferroni multiple comparisons to identify between group and time differences.²⁰ The nonparametric parameters or those with a sample size of <15 animals were compared by using Mann-Whitney test.²¹ The analyses were performed using SPSS for Windows version 20.0 software (IBM) and tabulated using Microsoft Excel 2003 software. The tests were performed with a 5% significance level.

RESULTS

Breast Cancer Provokes Physical Characteristic Changes

Body weight increased in both MMTV-PyMT⁻ and MMTV-PyMT⁺ mice (Figure S1, $P_{\text{time}} < 0.001$). Despite significant interaction ($P_{\text{interaction}} = 0.013$), it was not possible to identify difference between groups throughout the study. Body weight after euthanasia was higher in MMTV-PyMT⁺ mice ($P < 0.001$). This difference was caused by tumor burden, since body weight without tumor was similar between groups (Figure S1). Anterior tibial muscle, lung, and brown and white fat weight were not different between MMTV-PyMT⁺ and MMTV-PyMT⁻ mice. Soleus muscle and kidney weight was lower and liver and spleen weight were higher in MMTV-PyMT⁺ mice compared with MMTV-PyMT⁻ mice (Table S1).

Breast Cancer Changes Physical Capacity

Time to exhaustion ($P_{\text{interaction}} = 0.031$) and treadmill velocity ($P_{\text{interaction}} = 0.037$) in the maximal exercise test were significantly lower in the MMTV-PyMT⁺ mice. Distance in the maximal exercise test was statistically lower in the MMTV-PyMT⁺ mice ($P_{\text{group}} = 0.003$) regardless of the time evaluated. These results are summarized in Table 1.

Breast Cancer Alters Cardiac Morphology and Function

The pooled data (beginning and end of the study) of the LVEDD (PyMT⁻ pre: 0.185±0.019 and post: 0.168±0.01 mm/g versus PyMT⁺ pre: 0.177±0.014 and post: 0.151±0.014 mm/g [$P_{\text{group}} < 0.001$, $P_{\text{interaction}} = 0.417$]) and LVEDV (PyMT⁻ pre: 2.99±0.41 and post: 2.64±0.38 µL/g versus PyMT⁺ pre: 2.61±0.35 and post: 2.45±0.34 µL/g [$P_{\text{group}} = 0.003$, $P_{\text{interaction}} = 0.437$]) were lower in the MMTV-PyMT⁺ mice when compared with MMTV-PyMT⁻ mice (Figure 2). LVESD and LVESV were similar between MMTV-PyMT⁺ and MMTV-PyMT⁻ mice. The LA responses were statistically different between groups throughout the experimental

Table 1. Physical Capacity Obtained in the Maximal Exercise Test in MMTV-PyMT- and MMTV-PyMT+ Mice at the Beginning and End of Experimental Protocol

Variable	MMTV-PyMT-		MMTV-PyMT+		P_{Group}	P_{Time}	$P_{\text{Interaction}}$
	Pre	Post	Pre	Post			
Distance, m	703.4±128.5	599.1±224.7	653.1±95.9	384.9±187.6	0.003*	<0.001*	0.079
Time, min	35.9±3.4	32.9±6.2	34.6±2.5	25.7±6.4	0.001*	<0.001*	0.031*
Velocity, m/min	36.2±3.3	33.7±6.3	34.9±2.8	26.6±6.6	0.002*	<0.001*	0.037*

Generalized estimation equations with normal distribution and identity link function using AR(1) correlation matrix between evaluations. Values are expressed as means±SD. One mouse in the mouse mammary tumor virus–polyomavirus middle T antigen (MMTV-PyMT)- group and 1 mouse in the MMTV-PyMT+ group were not included in exercise tolerance test. The MMTV-PyMT- mouse refused to run on the treadmill, while the MMTV-PyMT+ mouse had its stride motion compromised by the tumor. Thus, 13 mice in the MMTV-PyMT- and 14 mice in the MMTV-PyMT+ groups were included in this study.

*Significant difference.

protocol ($P_{\text{interaction}}=0.004$). The comparison between groups showed that at the beginning of the study, the LA was not different between the MMTV-PyMT+ and MMTV-PyMT- groups; however, at the end of the study, the LA was lower in MMTV-PyMT+ mice (0.079 ± 0.001 versus 0.091 ± 0.008 mm/g, $P=0.030$) (Figure 2 and Table S2). The pooled data (beginning and end of the study) of LV mass was lower in MMTV-PyMT+ mice than in MMTV-PyMT- mice (PyMT- pre: 4.297 ± 0.798 and post: 3.396 ± 0.496 mg/g versus PyMT+ pre: 3.454 ± 0.649 and post: 2.968 ± 0.601 mg/g [$P_{\text{group}}<0.001$, $P_{\text{interaction}}=0.365$]) (Figure 2 and Table S2). E/E' wave, E-wave deceleration time, and IVRT values were not different between groups. Similarly, heart rate, fractional shortening, ejection fraction, and myocardium performance index were not different in MMTV-PyMT- and MMTV-PyMT+ mice.

Longitudinal strain and strain rate at the beginning and at the end of the study are shown in Figure 3. The pooled data (beginning and end of the study) of the longitudinal strain (PyMT- pre: -14.4 ± 4.8 and post: $-14.5\pm 2.7\%$ versus PyMT+ pre: -12.4 ± 2.4 and post: $-9.8\pm 1.7\%$ [$P_{\text{group}}<0.001$, $P_{\text{interaction}}=0.126$]) and strain rate (PyMT- pre: -5.07 ± 2.27 and post: -6.03 ± 3.56 s⁻¹ versus PyMT+ pre: -4.39 ± 1.47 and post: -3.66 ± 0.92 s⁻¹ [$P_{\text{group}}=0.030$, $P_{\text{interaction}}=0.168$]) were impaired in the MMTV-PyMT+ mice when compared with MMTV-PyMT- mice. Both the longitudinal strain and strain rate were statistically lower in absolute value in animals with cancer than in control animals. Radial strain and strain rate, radial and circumferential short systolic axis strain, and strain rate were similar between MMTV-PyMT- and MMTV-PyMT+ mice (Table S2).

Cardiac myocyte diameter and cardiac collagen volume fraction were similar between MMTV-PyMT- and MMTV-PyMT+ mice (Table 2).

Breast Cancer Changes Myocyte Ca²⁺-Handling Protein Expression

In an attempt to understand the molecular basis of the alterations in the longitudinal strain and strain rate in the

MMTV-PyMT+ mice at end of the study protocol, we studied Ca²⁺-handling proteins in the cardiac myocyte (Figure 4). In the MMTV-PyMT+ mice, phospholamban protein expression was increased (247.8% [IQR, 192.3%–360.4%] versus 105.4% [IQR, 76.8%–123.7%], $P=0.011$), whereas sodium/calcium exchanger protein expression was decreased (40.5% [IQR, 11%–66.6%] versus 101.5% [IQR, 64.2%–143.5%], $P=0.017$) compared with MMTV-PyMT- mice. SERCA2a protein expression was not different between the MMTV-PyMT+ and MMTV-PyMT- groups (51.1% [IQR, 37%–84.5%] versus 91.3% [IQR, 55.2%–159.7%], $P=0.165$); however, the SERCA2a/phospholamban ratio was reduced in the MMTV-PyMT+ mice (0.23% [IQR, 0.15%–0.61%] versus 0.86% [IQR, 0.65%–1.41%], $P=0.007$). We also observed that p-phospholamban was lower in the MMTV-PyMT+ compared with the MMTV-PyMT- mice (31.2% [IQR, 3.5%–69.6%] versus 83.8 [IQR, 47.9%–163.3%], $P=0.038$), but because of the lack of a sufficient sample we were able to test this marker only 2 times.

ET Does Not Reverse Morphologic and Physiologic Changes in MMTV-PyMT+ Mice and Does Not Delay Time to Tumor Growth

Next, we assessed the impact of ET in modulating the changes in exercise capacity, cardiac function, and tumor growth in the MMTV-PyMT+ mice. ET had no effect on tumor growth rate. Time of tumor growth to reach 1 cm³ was not significantly different between sedentary and exercise-trained mice (11.0 ± 1.3 versus 12.8 ± 0.6 weeks, $P=0.215$).

ET did not affect animal body weight (Figure S2; $P_{\text{interaction}}=0.930$) or weight of the heart, anterior tibial and soleus muscles, liver, spleen, kidneys, and brown and white fat (Table S3; $P>0.05$). ET did not seem to prevent the reduction in physical capacity provoked by cancer (Figure S3). There was a significant reduction in the distance covered in the ETTs performed during the experimental protocol in both groups

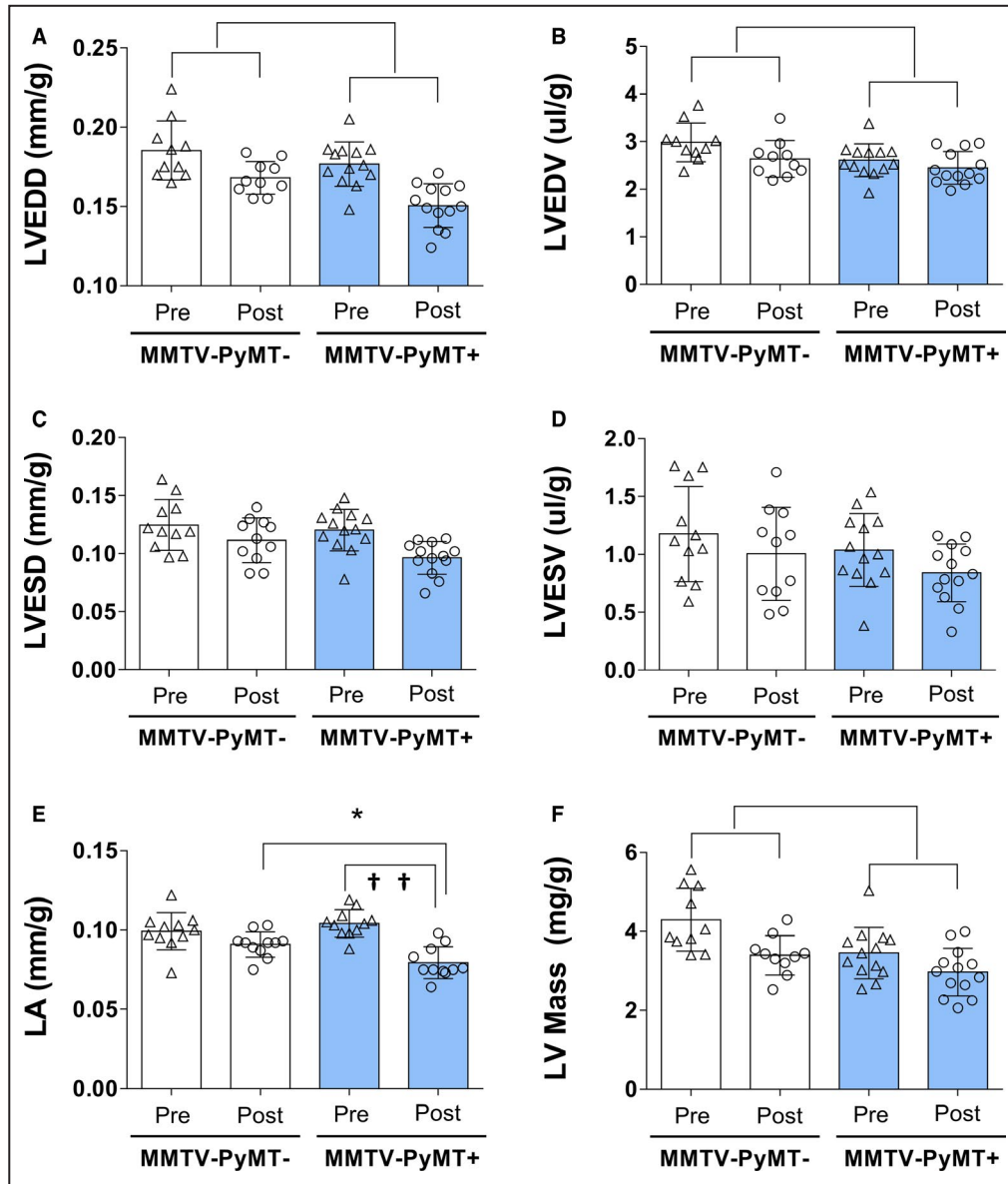


Figure 2. Morphological and functional cardiac parameters in mouse mammary tumor virus-polyomavirus middle T antigen (MMTV-PyMT)⁻ and MMTV-PyMT⁺ mice in the pre-experimental and post-experimental protocol.

Left-ventricular (LV) end-diastolic diameter (LVEDD) (A); LV end-diastolic volume (LVEDV) (B); LV end-systolic diameter (LVESD) (C); LV end-systolic volume (LVESV) (D); left atrium (LA) (E); and LV mass (F). Parameters were corrected by weight. LVEDD: $P_{\text{group}} < 0.001$, $P_{\text{interaction}} = 0.417$; LVEDV: $P_{\text{group}} = 0.003$, $P_{\text{interaction}} = 0.437$; LA: $P_{\text{interaction}} = 0.004$; post hoc test: $^*P = 0.030$, between group difference and $^{\dagger\dagger}P < 0.001$, within MMTV-PyMT⁺ group difference; and LV mass: $P_{\text{group}} < 0.001$, $P_{\text{interaction}} = 0.365$. Generalized estimation equations with normal distribution and identity link function using AR(1) correlation matrix between evaluations followed by Bonferroni multiple comparison. Values are expressed as means and SD. Four mice in the MMTV-PyMT⁻ and 2 mice in the MMTV-PyMT⁺ were excluded from this analysis because of poor imaging quality on echocardiography. Thus, 10 mice in the MMTV-PyMT⁻ and 13 mice in the MMTV-PyMT⁺ were involved in this analysis. Of note, 2 LA measures were not obtained in the MMTV-PyMT⁺ mice.

($P_{\text{time}} < 0.001$), although no significant difference in running distance was observed between the sedentary and exercise-trained groups at 0, 1, 2, and 3 months ($P_{\text{interaction}} = 0.069$). This occurred despite a significant

increase in citrate synthase enzyme activity in both anterior tibial and soleus muscle (Figure S4; $P < 0.001$).

Data of cardiac morphology and function in sedentary and exercise-trained MMTV-PyMT⁺ mice are

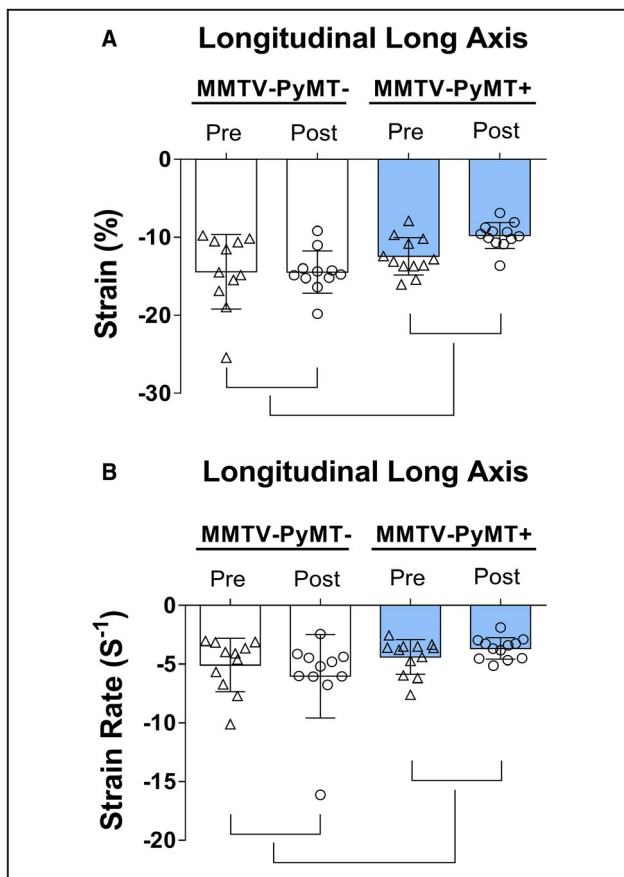


Figure 3. Cardiac function by speckle tracking in mouse mammary tumor virus–polyomavirus middle T antigen (MMTV-PyMT)⁻ and MMTV-PyMT⁺—longitudinal long-axis strain (A) and strain rate (B).

Longitudinal strain ($P_{\text{group}} < 0.001$, $P_{\text{interaction}} = 0.126$) and strain rate ($P_{\text{group}} = 0.030$, $P_{\text{interaction}} = 0.168$) were lower in MMTV-PyMT⁺ mice when compared with MMTV-PyMT⁻ mice. Pre: pre phase tumor growth and post: post phase tumor growth. Generalized estimation equations with normal distribution and identity link function using AR(1) correlation matrix between evaluations. Values are expressed as means and SD. Three mice in the MMTV-PyMT⁻ and 3 mice in the MMTV-PyMT⁺ groups were excluded from the speckle-tracking analysis because of poor imaging quality. Thus, 11 mice in the MMTV-PyMT⁻ and 12 mice in the MMTV-PyMT⁺ were involved in this analysis.

shown in Figure S5 and Table S4. ET decreased LVESD ($P_{\text{group}} = 0.038$, $P_{\text{interaction}} = 0.226$) and LVEDV ($P_{\text{group}} = 0.026$, $P_{\text{interaction}} = 0.431$), but did not change the other parameters associated with cardiac morphology (Table S4). Despite the average difference in longitudinal strain rate responses throughout the experimental protocol ($P_{\text{interaction}} = 0.032$; Table S4), it was not possible to identify differences between sedentary and exercise-trained MMTV-PyMT⁺ mice.

ET did not improve phospholamban protein expression. Likewise, ET did not change SERCA2a, p-phospholamban, and sodium-calcium exchanger protein expression. In addition, ET did not alter

SERCA2a/phospholamban ratio (Figure S6). Additional results can be found in Data S1.

DISCUSSION

Previous studies have shown that chemotherapy agents used for treatment of breast cancer are associated with cardiotoxicity.^{7,22} Changes in QT interval,^{6,23} ventricular arrhythmias,^{6,24} acute coronary syndrome,^{5,25} and systolic and diastolic LV dysfunction have been reported in patients undergoing chemotherapy. However, the impact of cancer progression in cardiovascular function remains poorly addressed. In this regard, our study shows for the first time that breast cancer itself, in an advanced stage, is associated with myocardial dysfunction. In MMTV-PyMT⁺ mice, we show that the presence of breast cancer was associated with worse longitudinal long-axis strain and strain rate, known subclinical markers of cardiac dysfunction, and impaired exercise capacity, both at least partly related to Ca²⁺protein-handling deregulation.

The evaluation of ventricular function by speckle-tracking imaging has been highly used in clinical practice. Ventricular longitudinal deformation alterations have been used for early detection of ventricular impairment before changes in circumferential and radial deformations in most cardiac diseases with high sensitivity and specificity.²⁶ In addition, longitudinal deformation changes are prognostic of cardiotoxicity²⁶ even in the presence of preserved ejection fraction.⁷ Our study shows for the first time that breast cancer is associated with impairment in LV longitudinal strain and strain rate, both consistent with subclinical myocardial dysfunction.²⁷ Furthermore, these myocardial alterations are associated with an increase in phospholamban expression and a decrease in sodium/calcium exchanger, p-phospholamban expression, and SERCA2a/phospholamban ratio in the cardiac myocyte of MMTV-PyMT⁺ mice, all consistent with altered myocardial Ca²⁺ handling. Ca²⁺-related proteins play an important role in myocardial contraction and relaxation. Phospholamban binds SERCA2a in a 1:1 heterodimeric regulatory complex, which results in inhibition of SERCA2a activity.^{28,29} Reduction in phosphorylation of phospholamban at Ser¹⁶ by protein kinase A and Thr¹⁷ by calmodulin-dependent protein kinase II increases the inhibition of phospholamban on SERCA2a.³⁰ These responses reduce Ca²⁺ reuptake into the sarcoplasmic reticulum during the muscle relaxation phase and the load of Ca²⁺ necessary for myocardial contraction in the subsequent cardiac cycle,³¹ which could explain the impairment in LV longitudinal strain and strain rate. Although our findings do not establish a definitive causal effect, they strongly suggest that Ca²⁺-handling deregulation

Table 2. Cardiac Morphology in MMTV-PyMT⁻ and MMTV-PyMT⁺

Variable	MMTV-PyMT ⁻		MMTV-PyMT ⁺		P Value
	Median (IQR)	N	Median (IQR)	N	
Myocyte diameter, μm	16.9 (15.8–20.7)	7	16.7 (16.3–18)	8	>0.999
Type 1 collagen, μm^2	339.3 (93.2–488.1)	7	381.7 (222.5–497.3)	7	0.535
Type 3 collagen, μm^2	403.4 (107–921.4)	7	902.5 (285–1000.8)	7	0.535
Type 1+3 collagen, μm^2	911 (194.9–1261.6)	7	1125 (621.2–1498.1)	7	0.383

Mann-Whitney test. Values are expressed as medians and interquartile range (IQR). MMTV-PyMT indicates mouse mammary tumor virus–polyomavirus middle T antigen.

plays at least a partial role in breast cancer–induced cardiac dysfunction.

Another important finding in our study was the association between breast cancer and changes to cardiac morphology. The reductions in LV diameter and volume associated with lower LV mass and LA size is suggestive of cardiac remodeling in consequence of breast cancer. These morphological changes can predispose to progression of ventricular dysfunction and malignant arrhythmias.³² Cancer cachexia has been associated with loss of cardiac mass and, consequently, cardiac dysfunction³³ and sarcopenia. The sarcopenia has been described in 25% of patients with metastatic breast cancer.^{34,35} In fact, we found decreased soleus muscle in MMTV-PyMT⁺ mice. Despite the changes in cardiac morphology, we found no changes in cardiomyocyte diameter and fibrosis. The histological adaptations related to heart mass loss seem to occur as a late compensation event, along with manifestations of overt clinical cardiac dysfunction, such as a fall in ejection fraction and fractional shortening.³³

Other than cardiac dysfunction, our findings in the MMTV-PyMT mouse model highlight that the systemic effects of cancer can affect other organs as well. Some findings include increased liver and spleen dimensions and decreased kidneys size compared with MMTV-PyMT⁻ mice. Despite no functional studies having been performed in these organs, hepatomegaly and kidney atrophy are well-established signs of organ dysfunction.^{36,37} In addition, splenomegaly has been associated with changes in immune function^{38,39} that can further affect the prognosis.⁴⁰ Spleen enlargement was associated with an increase in the percentage of CD3⁺T lymphocytes and CD8⁺T lymphocytes.⁴¹ Of note, ET did not impact the weight of these organs in MMTV-PyMT⁺ mice.

Our group has previously reported that ET improves the net balance of cardiac Ca²⁺-handling–related proteins in heart failure,⁴² and similar findings were observed in obese rat models.⁹ This improvement seems to be related to a reduction in cardiac phospho–Thr17-phospholamban and phospho–Ser2808-Ryanodine protein expression, which ultimately improves cardiac

function.⁹ Based on these findings, we hypothesized that ET would prevent cancer-induced cardiac dysfunction, but this was not the case. ET decreased LVESD and LVEDV, but physical capacity was not overall changed. Likewise, ET did not change cardiomyocyte Ca²⁺-handling protein expression. It is likely that the lack of anti-tumor effect of ET alone in the absence of specific anti-cancer therapy to halt cancer progression is at least partly if not completely associated with these findings. This is supported by the fact that ET alone did not impact the tumor growth rate in the MMTV-PyMT⁺ mice. Another possibility is that our exercise paradigm was not adequate to prevent the changes in cardiac function in MMTV-PyMT⁺ mice. Despite forced treadmill exercise being an accepted model of animal training, it may be insufficient or inadequate for animals with ongoing cancer progression. We are convinced that studies involving ET in cancer models should continue. However, we recognize that these studies should be performed in the context of anti-cancer treatment to understand how ET may synergize with specific anti-cancer therapies to promote cancer control and/or preservation of body homeostasis. This is an area of ongoing investigation in our group as well as others.

STUDY LIMITATIONS

The animals were euthanized when the tumor reached 1 cm³, ie, at the late stage of breast cancer. Thus, our study does not provide information on the effects of breast cancer on cardiac function during the development of the disease. The reduction in caveolin-1 following transformation of activated oncogenes, including the polyomavirus middle T antigen (PyMT),⁴³ and the known role of caveolin-1 in several cardiovascular alterations⁴⁴ could lead someone to raise the hypothesis that the cardiac alterations in the present study were due, in part, to the reduction in caveolin-1. The activation in mitogen-activated protein kinase (MAPK) and phosphoinositide 3-kinase (PI3K) pathways associated with PyMT^{45,46} might have also contributed to the cardiac alterations in the present study. The role of extracellular

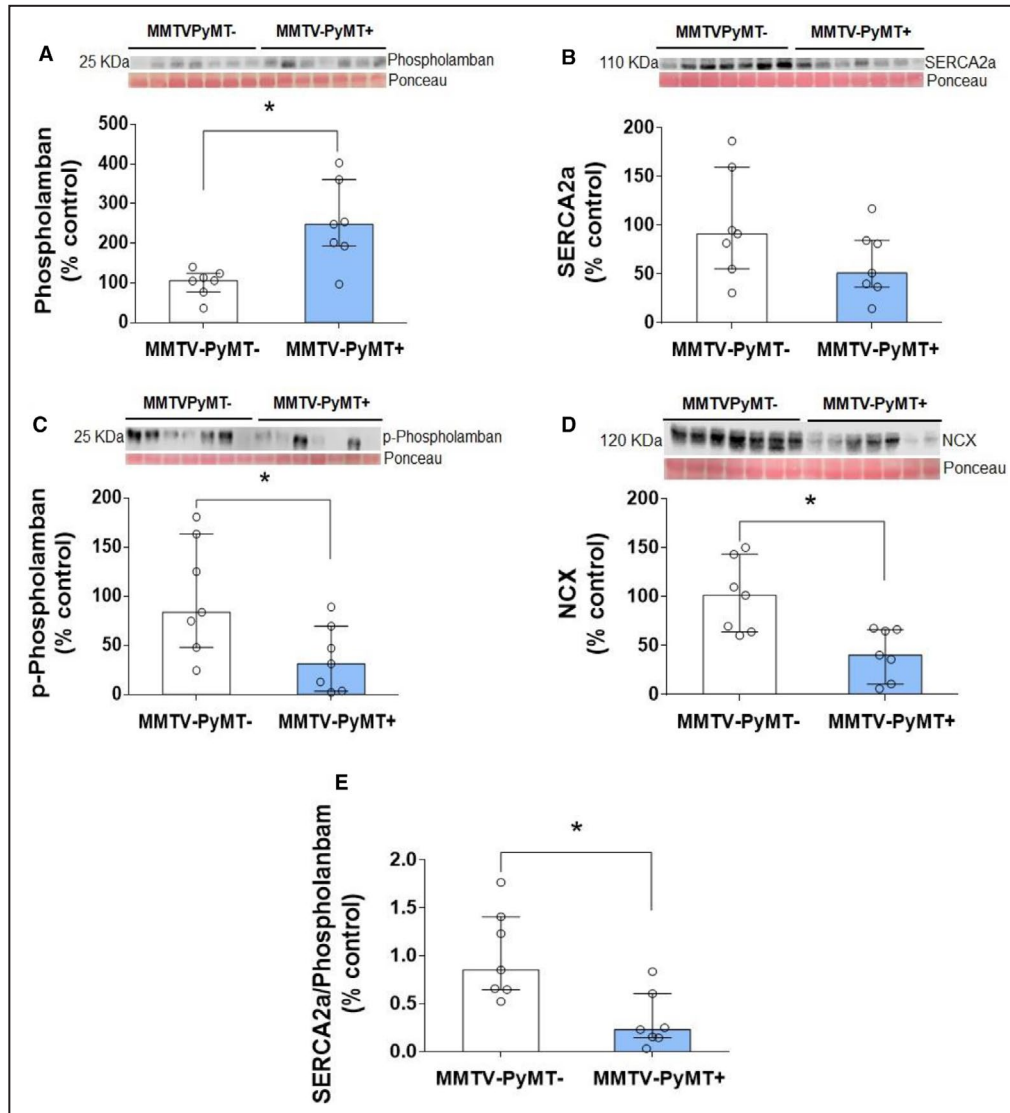


Figure 4. Cardiac myocyte Ca^{2+} -handling proteins in mouse mammary tumor virus–polyomavirus middle T antigen (MMTV-PyMT)⁻ and MMTV-PyMT⁺ mice—phospholamban (A); SERCA2a (sarcolemmal or endoplasmic reticulum calcium 2 ATPase) (B); phosphorilated phospholamban (p-phospholamban) (C); sodium/calcium exchanger (NCX) (D); and SERCA2a/phospholamban ratio (E).

Western blot bands are shown for each protein. In the MMTV-PyMT⁺ mice, phospholamban protein expression was increased ($P=0.011$) and SERCA2a protein expression was not different between the MMTV-PyMT⁺ and MMTV-PyMT⁻ groups ($P=0.165$). SERCA2a/phospholamban ratio was reduced in the MMTV-PyMT⁺ mice ($P=0.007$). p-Phospholamban and NCX protein expression were decreased ($P=0.038$ and $P=0.017$, respectively) compared with MMTV-PyMT⁻ mice. Mann-Whitney test. Values are expressed as medians and interquartile ranges (IQRs). Animals per group: 7 MMTV-PyMT⁻ and 7 MMTV-PyMT⁺.

signal-regulated kinase (ERK), c-Jun N-terminal kinase (JNK), and p38 MAPK has been established in animal models and humans with heart failure.^{47,48} The increase in total PI3K activity can negatively regulate Ca^{2+} transients, which results in decreasing of positive inotropic effects of β -adrenergic agonists.⁴⁹ Unfortunately, the caveolin-1, MAPK, and PI3K were not investigated in our study. This is an interesting topic for further investigations.

The study was entirely conducted in animals, which limits its extrapolation to humans with breast cancer. In addition, we analyzed a breast cancer model (MMTV-PyMT) that only resembles HER2-positive breast cancer in humans. Thus, our findings cannot be generalized to other tumor types. However, the MMTV-PyMT mouse is a unique transgenic model of multifocal breast adenocarcinoma because cancer development occurs similarly to that of invasive ductal carcinoma of the human

breast. Cancer spontaneously develops and gradually progresses from hyperplasia, dysplasia, adenoma, and carcinoma because of expression of the polyoma middle oncoprotein (PyMT).¹² Therefore, we believe that our study will provide important information that will be useful for future investigations in the clinical setting.

CONCLUSIONS

Breast cancer is associated with decreased exercise capacity and subclinical LV dysfunction in MMTV-PyMT-mice, which is directly associated with dysregulation of cardiomyocyte Ca²⁺-handling. ET alone is not an effective strategy to prevent or reverse these changes.

ARTICLE INFORMATION

Received June 16, 2020; accepted January 21, 2021.

Affiliations

From the Heart Institute (InCor) do Hospital das Clínicas, Faculdade de Medicina (T.S.d.C., U.U., C.P.J., C.S.P., I.L.G., V.M.S., L.A.H., R.K.F., C.E.N.), Cancer Institute of the State of São Paulo, Hospital das Clínicas, Faculdade de Medicina (T.S.d.C., L.A.H., R.C.) and School of Physical Education and Sport (U.U., P.C.B., E.M.O., C.E.N.), Universidade de São Paulo, Brasil; Department of Thoracic/Head and Neck Medical Oncology, The University of Texas, MD Anderson Cancer Center, Houston, TX (M.V.N.); Edwin L. Steele Laboratories for Tumor Biology, Department of Radiation Oncology, Massachusetts General Hospital & Harvard Medical School, Boston, MA (I.L.G.); and Centro de Oncologia Molecular, Hospital Sírio-Libanês, São Paulo, Brazil (A.A.C.).

Sources of Funding

This work was supported by the Fundação de Amparo à Pesquisa do Estado de São Paulo (FAPESP#2015/22814-5). Gomes-Santos and Passos received scholarship from FAPESP (#2014/13690-8 and #15/19076-2, respectively). Brum, Oliveira, Salemi and C. E. Negrão were supported by Conselho Nacional de Desenvolvimento Científico e Tecnológico (CNPQ#306261/2016-2; #313479/2017-8; #307227/2018-9 and; #303573/2015-5).

Disclosures

None.

Supplementary Material

Data S1

Tables S1–S4

Figures S1–S6

REFERENCES

- GLOBOCAN 2020: new global cancer data|UICC. Available at: <https://www.uicc.org/news/globocan-2020-new-global-cancer-data>. Accessed January 13, 2021.
- Kesson EM, Allardice GM, George WD, Burns HJG, Morrison DS. Effects of multidisciplinary team working on breast cancer survival: retrospective, comparative, interventional cohort study of 13 722 women. *BMJ*. 2012;344:e2718. DOI: 10.1136/bmj.e2718.
- Moslehi JJ. Cardiovascular toxic effects of targeted cancer therapies. *New Engl J Med*. 2016;375:1457–1467. DOI: 10.1056/NEJMr1100265.
- Chow AY, Chin C, Dahl G, Rosenthal DN. Anthracyclines cause endothelial injury in pediatric cancer patients: a pilot study. *J Clin Oncol*. 2006;24:925–928. DOI: 10.1200/JCO.2005.03.5956.
- Herrmann J, Yang EH, Ilescu CA, Marmagkiolis K. Response by Herrmann et al. to Letter Regarding Article, “vascular toxicities of cancer therapies: the old and the new—an evolving avenue”. *Circulation*. 2016;133:1272–1289. DOI: 10.1161/CIRCULATIONAHA.115.018347.
- Buza V, Rajagopalan B, Curtis AB. Cancer treatment-induced arrhythmias: focus on chemotherapy and targeted therapies. *Circ Arrhythm Electrophysiol*. 2017;10:1–13. DOI: 10.1161/CIRCEP.117.005443.
- Bloom MW, Hamo CE, Cardinale D, Ky B, Nohria A, Baer L, Skopicki H, Lenihan DJ, Gheorghiu M, Lyon AR, et al. Cancer therapy-related cardiac dysfunction and heart failure part 1: definitions, pathophysiology, risk factors, and imaging. *Circ Hear Fail*. 2017;9:1–21.
- Hershman DL, Till C, Shen S, Wright JD, Ramsey SD, Barlow WE, Unger JM. Association of cardiovascular risk factors with cardiac events and survival outcomes among patients with breast cancer enrolled in SWOG clinical trials. *J Clin Oncol*. 2018;36:2710–2717. DOI: 10.1200/JCO.2017.77.4414.
- Paulino EC, Ferreira JC, Bechara LR, Tsutsui JM, Mathias W, Lima FB, Casarini DE, Cicogna AC, Brum PC, Negrão CE. Exercise training and caloric restriction prevent reduction in cardiac Ca²⁺-handling protein profile in obese rats. *Hypertension*. 2010;56:629–635.
- Medeiros A, Rolim NPL, Oliveira RSF, Rosa KT, Mattos KC, Casarini DE, Irigoyen MC, Krieger EM, Krieger JE, Negrão CE, et al. Exercise training delays cardiac dysfunction and prevents calcium handling abnormalities in sympathetic hyperactivity-induced heart failure mice. *J Appl Physiol*. 2008;104:103–109. DOI: 10.1152/jappphysiol.00493.2007.
- Duivenvoorden HM, Spurling A, O’Toole SA, Parker BS. Discriminating the earliest stages of mammary carcinoma using myoepithelial and proliferative markers. *PLoS One*. 2018;13:1–12. DOI: 10.1371/journal.pone.0201370.
- Lin EY, Jones JG, Li P, Zhu L, Whitney KD, Muller WJ, Pollard JW. Progression to malignancy in the polyoma middle T oncoprotein mouse breast cancer model provides a reliable model for human diseases. *Am J Pathol*. 2003;163:2113–2126. DOI: 10.1016/S0002-9440(10)63568-7.
- Park MK, Lee CH, Lee H. Mouse models of breast cancer in pre-clinical research. *Lab Anim Res*. 2018;34:160–165. DOI: 10.5625/lar.2018.34.4.160.
- Eckelman WC, Kilbourn MR, Joyal JL, Labiris R, Valliant JF. Justifying the number of animals for each experiment. *Nucl Med Biol*. 2007;34:229–232. DOI: 10.1016/j.nucmedbio.2007.01.005.
- Parkins KM, Dubois VP, Hamilton AM, Makela AV, Ronald JA, Foster PJ. Multimodality cellular and molecular imaging of concomitant tumour enhancement in a syngeneic mouse model of breast cancer metastasis. *Sci Rep*. 2018;8:1–10. DOI: 10.1038/s41598-018-27208-4.
- Ferreira JC, Rolim NP, Bartholomeu JB, Gobatto CA, Kokubun E, Brum PC. Maximal lactate steady state in running mice: effect of exercise training. *Clin Exp Pharmacol Physiol*. 2007;34:760–765. DOI: 10.1111/j.1440-1681.2007.04635.x.
- Salemi VM, Bilate AM, Ramires FJ, Picard MH, Gregio DM, Kalil J, Neto EC, Mady C. Reference values from M-mode and Doppler echocardiography for normal Syrian hamsters. *Eur J Echocardiogr*. 2005;6:41–46. DOI: 10.1016/j.euje.2004.06.001.
- De Lucia C, Wallner M, Eaton DM, Zhao H, Houser SR, Koch WJ. Echocardiographic strain analysis for the early detection of left ventricular systolic/diastolic dysfunction and dyssynchrony in a mouse model of physiological aging. *J Gerontol A Biol Sci Med Sci*. 2019;74:455–461. DOI: 10.1093/gerona/gly139.
- McCullagh P, Nelder JA. *Generalized Linear Models*. 2nd ed. London, England: Chapman and Hall; 1989:1–532.
- Neter J, Kutner M, Wasserman W, Nachtsheim C. *Applied Linear Statistical Models*. 4th ed. New York, NY: McGraw-Hill; 1996:1–1408.
- Kirkwood BR, Sterne JA. *Essential Medical Statistics*. 2nd ed. New York, NY: John Wiley & Sons; 2003:1–512.
- Jones LW, Haykowsky MJ, Swartz JJ, Douglas PS, Mackey JR. Early breast cancer therapy and cardiovascular injury. *J Am Coll Cardiol*. 2007;50:1435–1441. DOI: 10.1016/j.jacc.2007.06.037.
- Accordino MK, Neugut AI, Hershman DL. Cardiac effects of anticancer therapy in the elderly. *J Clin Oncol*. 2014;32:2654–2661. DOI: 10.1200/JCO.2013.55.0459.
- Farmakis D, Parissis J, Filippatos G. Insights into onco-cardiology: atrial fibrillation in cancer. *J Am Coll Cardiol*. 2014;63:945–953. DOI: 10.1016/j.jacc.2013.11.026.
- Peretto G, Lazzeroni D, Sartorio CL, Camici PG. Cardiotoxicity in oncology and coronary microcirculation: future challenges in theranostics. *Front Biosci (Landmark Ed)*. 2017;22:1760–1773.
- Negishi K, Negishi T, Hare JL, Haluska BA, Plana JC, Marwick TH. Independent and incremental value of deformation indices for prediction of trastuzumab-induced cardiotoxicity. *J Am Soc Echocardiogr*. 2013;26:493–498. DOI: 10.1016/j.echo.2013.02.008.

27. Nahum J, Bensaid A, Dussault C, Macron L, Clémence D, Bouhemad B, Monin JL, Rande JL, Gueret P, Lim P. Impact of longitudinal myocardial deformation on the prognosis of chronic heart failure patients. *Circ Cardiovasc Imaging*. 2010;3:249–256. DOI: 10.1161/CIRCIMAGING.109.910893.
28. Cantilina T, Sagara Y, Inesi G, Jones LR. Comparative studies of cardiac and skeletal sarcoplasmic reticulum ATPases. *J Biol Chem*. 1993;268:17018–17025.
29. Sasaki T, Inui M, Kimura Y, Kuzuya T, Tada M. Molecular regulation of Ca²⁺ pump ATPase by phospholamban in cardiac sarcoplasmic reticulum. *J Biol Chem*. 1992;267:1674–1679.
30. Mattiazzi A, Mundiña-Weilenmann C, Guoxiang C, Vittone L, Kranias E. Role of phospholamban phosphorylation on Thr17 in cardiac physiological and pathological conditions. *Cardiovasc Res*. 2005;68:366–375. DOI: 10.1016/j.cardiores.2005.08.010.
31. Díaz ME, Graham HK, O'Neill SC, Trafford AW, Eisner DA. The control of sarcoplasmic reticulum Ca content in cardiac muscle. *Cell Calcium*. 2005;38:391–396. DOI: 10.1016/j.ceca.2005.06.017.
32. Azevedo PS, Polegato BF, Minicucci MF, Paiva SA, Zornoff LA. Cardiac remodeling: concepts, clinical impact, pathophysiological mechanisms and pharmacologic treatment. *Arq Bras Cardiol*. 2016;106:62–69. DOI: 10.5935/abc.20160005.
33. Springer J, Tschirner A, Haghikia A, von Haehling S, Lal H, Grzesiak A, Kaschina E, Palus S, Pötsch M, von Websky K, et al. Prevention of liver cancer cachexia-induced cardiac wasting and heart failure. *Eur Heart J*. 2014;35:932–941. DOI: 10.1093/eurheartj/eh302.
34. Wang R, Bhat-nakshatri P, Padua MB, Prasad MS, Anjanappa M, Jacobson M, Finnearty C, Sefcsik V, McElyea K, Redmond R, et al. Pharmacological dual inhibition of tumor and tumor-induced functional limitations in transgenic model of breast cancer. *Mol Cancer Ther*. 2017;16:2747–2758.
35. Rossi F, Valdora F, Bignotti B, Torri L, Succio G, Tagliacchio AS. Evaluation of body computed tomography-determined sarcopenia in breast cancer patients and clinical outcomes: a systematic review. *Cancer Treat Res Commun*. 2019;21:1–7. DOI: 10.1016/j.ctarc.2019.100154.
36. Collett JA, Paulose JK, Cassone VM, Osborn JL. Kidney-specific reduction of oxidative phosphorylation genes derived from spontaneously hypertensive rat. *PLoS One*. 2015;10:1–19. DOI: 10.1371/journal.pone.0136441.
37. Goncalvesová E. [Liver in heart failure]. *Vnitr Lek*. 2014;60:298–303.
38. Mu J, Jeyanathan M, Shaler CR, Horvath C, Damjanovic D, Zganiacz A, Kugathasan K, McCormick S, Xing Z. Respiratory mucosal immunization with adenovirus gene transfer vector induces helper CD4 T cell-independent protective immunity. *J Gene Med*. 2010;12:693–704. DOI: 10.1002/jgm.1487.
39. Zanetti M, Castiglioni P, Ingulli E. Principles of memory CD8 T-cells generation in relation to protective immunity. *Adv Exp Med Biol*. 2010;684:108–125.
40. Marshall JC, Charbonney E, Gonzalez PD. The immune system in critical illness. *Clin Chest Med*. 2008;29:605–616. DOI: 10.1016/j.ccm.2008.08.001.
41. Fang JJ, Zhu ZY, Dong H, Zheng GQ, Teng AG, Liu AJ. Effect of spleen lymphocytes on the splenomegaly in hepatocellular carcinoma-bearing mice. *Biomed Environ Sci*. 2014;27:17–26.
42. Rolim NPL, Medeiros A, Rosa KT, Mattos KC, Irigoyen MC, Krieger EM, Krieger JE, Negrão CE, Brum PC. Exercise training improves the net balance of cardiac Ca²⁺ handling protein expression in heart failure. *Physiol Genomics*. 2007;29:246–252.
43. Koleske AJ, Baltimore D, Lisanti MP. Reduction of caveolin and caveolae in oncogenically transformed cells. *Proc Natl Acad Sci USA*. 1995;92:1381–1385. DOI: 10.1073/pnas.92.5.1381.
44. Wunderlich C, Schober K, Lange SA, Drab M, Braun-Dullaues RC, Kasper M, Schwencke C, Schmeisser A, Strasser RH. Disruption of caveolin-1 leads to enhanced nitrosative stress and severe systolic and diastolic heart failure. *Biochem Biophys Res Commun*. 2006;340:702–708. DOI: 10.1016/j.bbrc.2005.12.058.
45. Wada M, Canals D, Adada M, Coant N, Salama MF, Helke KL, Arthur JS, Shroyer KR, Kitatani K, Obeid LM, et al. P38 delta MAPK promotes breast cancer progression and lung metastasis by enhancing cell proliferation and cell detachment Masayuki. *Oncogene*. 2018;36:6649–6657. DOI: 10.1038/onc.2017.274.
46. Sai J, Owens P, Novitskiy SV, Hawkins OE, Vilgelm AE, Yang J, Sobolik T, Lavender N, Johnson AC, McClain C, et al. PI3K inhibition reduces mammary tumor growth and facilitates anti-tumor immunity and anti-PD1 responses. *Clin Cancer Res*. 2018;23:3371–3384. DOI: 10.1158/1078-0432.CCR-16-2142.
47. Haq S, Choukroun G, Lim H, Tymitz KM, del Monte F, Gwathmey J, Grazette L, Michael A, Hajjar R, Force T, et al. Differential activation of signal transduction pathways in human hearts with hypertrophy versus advanced heart failure. *Circulation*. 2001;103:670–677. DOI: 10.1161/01.CIR.103.5.670.
48. Muslin AJ. MAPK signaling in cardiovascular health and disease: molecular mechanisms and therapeutic targets. *Clin Sci*. 2009;115:203–218.
49. Ghigo A, Laffargue M, Li M, Hirsch E. PI3K and calcium signaling in cardiovascular disease. *Circ Res*. 2017;121:282–292. DOI: 10.1161/CIRCRESAHA.117.310183.

SUPPLEMENTAL MATERIAL

Data S1.

SUPPLEMENTAL RESULTS

Impact of Breast Cancer

Breast cancer provokes physical characteristic changes

Body weight in MMTV-PyMT⁺ and MMTV-PyMT⁻ mice is shown in **Figure S1**. Body weight increased in both MMTV-PyMT⁻ and MMTV-PyMT⁺ mice (p-time<0.001). Despite of significant interaction (p=0.013), it was not possible to identify the difference between groups throughout the study. Body weight after euthanasia was higher in MMTV-PyMT⁺ mice (p<0.001). This difference was due to tumor burden, since body weight without tumor was similar between groups.

Values of organs and tissues are shown in **Table S1**. Observe that anterior tibial muscle, lung and brown and white fat weight were not different between MMTV-PyMT⁻ and MMTV-PyMT⁺ mice, liver and spleen were greater in MMTV-PyMT⁺ mice, while kidney and soleus muscle were lower in MMTV-PyMT⁺ mice.

Breast cancer alters cardiac morphology and function

All cardiac function and morphology parameters analyzed are shown in **Table S2**. The pooled data (beginning and end of the study) of the LVEDD (PyMT⁻ pre and post vs. PyMT⁺ pre and post; p-group<0.001, p-interaction=0.417) and LVEDV (PyMT⁻ pre and post vs. PyMT⁺ pre and post; p-group=0.003, p-interaction=0.437) were lower in the MMTV-PyMT⁺ mice when compared to MMTV-PyMT⁻. LVESD and LVESV were similar between MMTV-PyMT⁻ and MMTV-PyMT⁺ mice. The left atrium responses were statistically different between groups throughout the experimental protocol (p-interaction=0.004). At the beginning of the study, the left atrium was not different between MMTV-PyMT⁺ and MMTV-PyMT⁻;

however, at the end of the study, the left atrium was lower in MMTV- PyMT+ mice (0.079 ± 0.001 vs. 0.091 ± 0.008 mm/g, $p=0.030$) (**Table S2**). The pooled data (beginning and end of the study) of the left ventricular mass was lower in MMTV-PyMT+ mice than in MMTV-PyMT- mice (PyMT- pre: 4.297 ± 0.798 and post: 3.396 ± 0.496 vs. PyMT+ pre: 3.454 ± 0.649 and post: 2.968 ± 0.601 mg/g, $p\text{-group}<0.001$, $p\text{-interaction}=0.365$). E/E' wave, E-wave deceleration time and IVRT values were not different between groups. Similarly, heart rate, fractional shortening, ejection fraction and myocardium performance index were not different in MMTV-PyMT- and MMTV-PyMT+ mice.

Longitudinal strain and strain rate at the beginning and at the end of the study are shown in **Table S2**. The pooled data (beginning and end of the study) of the longitudinal strain (PyMT- pre and post vs. PyMT+ pre and post, $p\text{-group}<0.001$, $p\text{-interaction}=0.126$) and strain rate (PyMT_ pre and post vs. PyMT+ pre and post, $p\text{-group}=0.030$, $p\text{-interaction}=0.168$) were impaired in the MMTV-PyMT+ mice when compared to MMTV-PyMT- mice. Both longitudinal strain and strain rate were statistically lower in absolute value in animals with cancer than in control animals. Radial strain and strain rate as well as radial and circumferential short systolic axis were similar between groups.

Exercise training does not reverse morphologic and physiologic changes in MMTV-PyMT+ mice, and does not delay time to tumor growth

Exercise training did not change body weight (**Figure S2**, $p\text{-interaction}=0.930$) and organs and tissues weight (**Table S3**, $p>0.05$). Also, ET did not influence tumor growth.

Exercise training did not prevent the decline in exercise tolerance (**Figure S3**, $p=0.069$), despite the increase in citrate synthase activity in the anterior tibial and soleus muscles (**Figure S4**, $p<0.001$).

Individual data of cardiac morphology and function in sedentary and exercise-trained MMTV-PyMT+ mice are shown in **Figure S5**. Exercise training decreased LVESD (p -

group=0.038, p-interaction=0.226) and LVEDV (p-group=0.026, p-interaction=0.431), but did not change the other parameters associated with cardiac morphology (**Table S4**). Despite the average difference in longitudinal strain rate responses throughout the experimental protocol (p-interaction=0.032, **Table S4**), it was not possible to identify differences between sedentary and exercise-trained MMTV-PyMT+ mice.

Exercise training did not improve phospholamban (p=0.006) and did not change SERCA2a (p=0.345), p-phospholamban (p=0.554), NCX (p=0.247) and SERCA2a/phospholamban (p=0.111) (**Figure S6**).

Table S1. Organ, tissue and tumor weight in MMTV-PyMT- and MMTV-PyMT+.

Variable	MMTV-PyMT-		MMTV-PyMT+		P
	median (IQR)	N	median (IQR)	N	
Anterior tibial	0.039 (0.036; 0.041)	12	0.036 (0.033; 0.039)	14	0.060
Soleus	0.007 (0.007; 0.007)	14	0.006 (0.006; 0.007)	15	0.029
Lung	0.15 (0.14; 0.17)	14	0.15 (0.14; 0.16)	15	0.983
Liver	0.98 (0.94; 1.04)	14	1.24 (1.16; 1.37)	15	<0.001
Spleen	0.069 (0.06; 0.081)	14	0.121 (0.094; 0.147)	15	<0.001
Kidney	0.26 (0.25; 0.28)	14	0.23 (0.22; 0.25)	15	0.001
Brown fat	0.063 (0.046; 0.082)	13	0.057 (0.042; 0.08)	14	0.583
White fat	0.15 (0.13; 0.2)	13	0.12 (0.09; 0.16)	14	0.068
Breast tumor			1.41 (1.22; 1.56)	15	
All tumors			2.95 (2.55; 4.64)	15	

Mann-Whitney's test. Values are expressed as medians and interquartile ranges (IQR). Anterior tibial was not collected in two mice in the MMTV-PyMT- group and brown and white fats were not collected in one mouse in the MMTV-PyMT- group and one mouse in the MMTV-PyMT+ group.

Table S2. Morphological and functional cardiac parameters in MMTV-PyMT- and MMTV-PyMT+ mice in the pre and post experimental protocol.

Variable	MMTV-PyMT-		MMTV-PyMT+		P Group	P Time	P Interaction
	pre	post	pre	post			
Morphology							
LVEDD/weight (mm/g)	0.185±0.019	0.168±0.01	0.177±0.014	0.151±0.014	<0.001	<0.001	0.417
LVESD/weight (mm/g)	0.125±0.022	0.112±0.019	0.12±0.018	0.096±0.014	0.060	0.001	0.309
LV Mass/weight (mg/g)	4.297±0.798	3.396±0.496	3.454±0.649	2.968±0.601	<0.001	0.002	0.365
LA/weight (mm/g)	0.099±0.012	0.091±0.008	0.104±0.008	0.079±0.01	0.270	<0.001	0.004
Volumes							
LVEDV/weight (µl/g)	2.99±0.41	2.64±0.38	2.61±0.35	2.45±0.34	0.003	0.039	0.437
LVESV/weight (µl/g)	1.18±0.41	1.01±0.4	1.04±0.31	0.84±0.25	0.132	0.063	0.897
Functional							
FS (%)	33.5±6.7	34.8±7.8	32.2±6.6	36.1±6.7	0.995	0.220	0.532
EF (%)	62.4±8.8	64.1±10.4	60.8±9.1	66±8.4	0.946	0.232	0.539
Ewave DECC (ms)	1.36±0.55	1.37±0.52	1.21±0.41	1.38±0.5	0.568	0.547	0.618
IVRTc (ms)	1.46±0.13	1.59±0.23	1.52±0.29	1.49±0.25	0.707	0.538	0.334
E/E' nor	28.4±5	26.1±5.9	28.3±6.3	26.7±6.5	0.876	0.376	0.871
HR (bpm)	417.6±29.9	435.3±40.5	400.9±44.9	427.5±37.7	0.260	0.046	0.687
MPI	15.6±2.8	14.6±2.3	15.8±2.1	14.8±3.5	0.761	0.245	0.971
RLA Strain	18.4±4.6	16.1±6.4	20.2±7.1	15.9±3.9	0.667	0.034	0.520
RLA Strain Rate	4.82±1.16	4.72±1.21	4.37±1.14	4.3±1.29	0.249	0.806	0.967
LLA Strain	-14.4±4.8	-14.5±2.7	-12.4±2.4	-9.8±1.7	<0.001	0.137	0.126
LLA Strain Rate	-5.07±2.27	-6.03±3.56	-4.39±1.47	-3.66±0.92	0.030	0.852	0.168
RSA Strain	21.9±8.6	20.1±8	23.6±9.8	22.2±6.4	0.517	0.423	0.926
RSA Strain Rate	5.45±1.5	5.15±1.22	4.88±1.37	5.28±1.3	0.619	0.899	0.331
CSA Strain	-17.9±2.7	-16.5±3.8	-17.5±4.9	-18.9±3	0.446	0.984	0.129
CSA Strain Rate	-5.57±1.16	-4.96±1.3	-5.28±1.44	-5.41±0.51	0.834	0.417	0.218

Left ventricle end diastolic diameter (LVEDD), left ventricle end systolic diameter (LVESD), left ventricle mass (LV), Left atrium (LA), left ventricle end diastolic volume (LVEDV) and left ventricle end systolic volume (LVESV). E wave (E), E wave deceleration time corrected (E wave DECc.) and isovolumetric relaxation time corrected (IVRTc), heart rate (HR), E' wave (E'), ejection fraction (EF), fractional shortening (FS), myocardium performance index (MPI), radial long axis (RLA), longitudinal long axis (LLA), radial short axis (RSA), circumferential short axis (CSA). The morphological parameters and volumes were corrected for weight. E wave DECc. and IVRTc were corrected for heart rate. GEE with normal distribution and identity link function using AR(1) correlation matrix between evaluations. Values are expressed as means \pm SD. Four mice in the MMTV-PyMT⁻ and 2 mice in the MMTV-PyMT⁺ were excluded from this analysis because of poor imaging quality in the echocardiography. Thus, 10 mice in the MMTV-PyMT⁻ and 13 mice in the MMTV-PyMT⁺ were involved in this analysis. Of note, two left atrium measures were not obtained in the MMTV-PyMT⁺ mice.

Table S3. Organs, tissues and tumor weight in sedentary and exercise-trained MMTV-PyMT+ mice.

Variable	Sedentary		Exercise-trained		p
	median (IQR)	N	median (IQR)	N	
Heart	0.116 (0.11; 0.124)	6	0.113 (0.105; 0.148)	6	0.937
Anterior tibial	0.036 (0.033; 0.039)	6	0.029 (0.026; 0.037)	6	0.180
Soleus	0.006 (0.006; 0.007)	6	0.006 (0.005; 0.006)	6	0.394
Liver	1.14 (1.08; 1.27)	6	1.21 (1.12; 1.28)	6	0.699
Spleen	0.15 (0.077; 0.183)	6	0.095 (0.088; 0.13)	6	0.485
Kidney	0.222 (0.204; 0.241)	6	0.219 (0.198; 0.227)	6	0.589
Brown fat	0.027 (0.015; 0.032)	6	0.025 (0.018; 0.034)	6	0.937
White fat	0.131 (0.075; 0.149)	6	0.128 (0.055; 0.222)	6	0.937
Breast tumor	1.53 (1.5; 2.35)	7	1.59 (1.09; 2.08)	10	0.475
All tumors	3.45 (2.37; 4.33)	8	3.2 (1.53; 5.29)	10	0.696

Mann-Whitney's test. Values are expressed as medians and interquartile ranges (IQR).

Table S4. Morphological and functional cardiac parameters in sedentary and exercise-trained MMTV-PyMT+ mice in the pre and post experimental protocol.

Variable	Sedentary		Exercise-trained		p Group	p Time	p Interaction
	Pre	Post	Pre	Post			
Morphology							
LVEDD/weight (mm/g)	0.182±0.018	0.161±0.016	0.175±0.013	0.148±0.013	0.084	<0.001	0.367
LVESD/weight (mm/g)	0.12±0.017	0.111±0.011	0.113±0.016	0.094±0.017	0.038	0.001	0.226
LV Mass/weight (mg/g)	3.875±0.939	3.726±0.861	3.392±0.533	3.284±0.613	0.062	0.549	0.925
LA/weight (mm/g)	0.103±0.007	0.088±0.009	0.1±0.014	0.089±0.006	0.780	<0.001	0.456
Volumes							
LVEDV/weight (µl/g)	2.84±0.58	2.72±0.5	2.48±0.35	2.2±0.54	0.026	0.058	0.431
LVESV/weight (µl/g)	1.05±0.33	1.11±0.2	0.89±0.31	1.03±0.56	0.350	0.452	0.765
Functional							
FS (%)	34.1±5.1	30.9±2.8	35.4±6.2	39±11.6	0.109	0.922	0.080
EF (%)	63.6±7.1	59.1±3.9	65.5±8.2	63±16.4	0.417	0.291	0.763
Ewave DECC (ms)	1.75±0.61	1.29±0.33	1.7±0.67	1.43±0.5	0.821	0.018	0.558
IVRTc (ms)	1.69±0.21	1.55±0.2	1.55±0.15	1.55±0.23	0.207	0.352	0.313
E/E' nor	31.1±6.4	26.8±4.1	27.4±6.7	31.3±11.2	0.893	0.914	0.069
HR (bpm)	399.3±45.4	424.4±25.3	413.4±56.7	433.4±19.6	0.360	0.091	0.848
MPI	13.7±2.3	14.6±4.4	13.2±1.8	13.1±1.4	0.264	0.620	0.594
RLA Strain	18.4±8.2	15.5±6.4	18.4±5.4	16.4±6.3	0.812	0.302	0.830
RLA Strain Rate	5.58±2.86	4.54±1.18	4.53±1.27	5.2±1.87	0.783	0.720	0.095
LLA Strain	-14.2±2.7	-11.4±3.1	-13±3.8	-16.4±6	0.117	0.838	0.055
LLA Strain Rate	-5.03±2.12	-3.76±1.51	-4.41±1.48	-5.75±2.2	0.265	0.957	0.032
RSA Strain	26±7.1	21.9±10.5	18.2±7	21.1±9.8	0.092	0.848	0.280
RSA Strain Rate	5.66±1.49	4.94±1.44	4.33±1.03	5.51±1.48	0.263	0.669	0.080
CSA Strain	-19.4±2.4	-17±4.1	-16.3±2.8	-17.4±4.1	0.235	0.581	0.144
CSA Strain Rate	-5.38±0.61	-4.75±0.75	-4.54±0.67	-5.02±1.13	0.223	0.823	0.093

Left ventricle end diastolic diameter (LVEDD), left ventricle end systolic diameter (LVESD), left ventricle mass (LV), Left atrium (LA), left ventricle end diastolic volume (LVEDV) and left ventricle end systolic volume (LVESV). E wave (E), E wave deceleration time corrected (E wave DECc), isovolumetric relaxation time corrected (IVRTc), heart rate (HR), E' wave (E'), ejection fraction (EF), fractional shortening (FS), myocardium performance index (MPI), radial long axis (RLA), longitudinal long axis (LLA), radial short axis (RSA), circumferential short axis (CSA). The morphological parameters and volumes were corrected by weight. E wave DECc. and IVRTc were corrected for heart rate. GEE with normal distribution and identity link function using AR(1) correlation matrix between evaluations. Values are expressed as means \pm SD. Two measurements of LVESV in MMTV-PyMT+ mice, and one measure of LA in each group were not obtained.

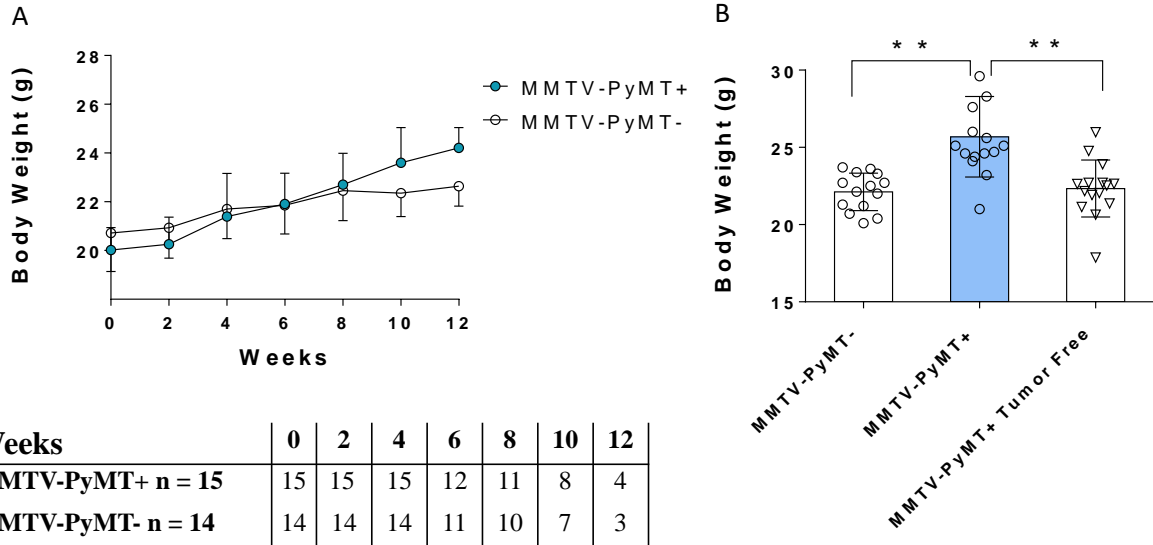
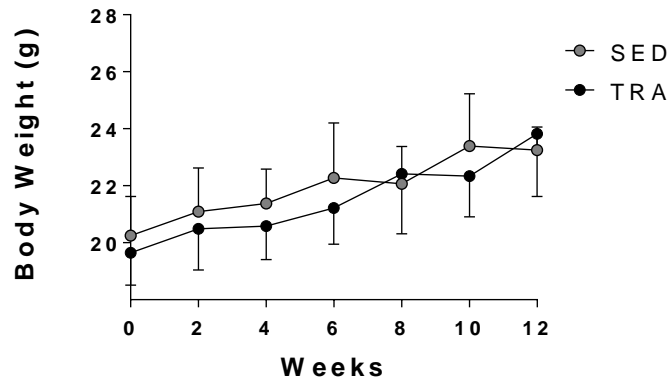


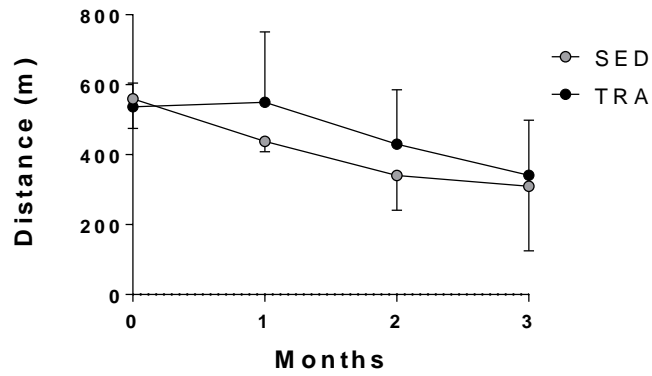
Figure S1. Body weight of MMTV-PyMT- and MMTV-PyMT+. The greater body weight in the MMTV-PyMT+ mice can be attributed to the increase in the volume of tumors.

(A) Evolution of body weight during experimental protocol. Numbers in the table means number of mice throughout the weeks. (B) Body weight after euthanasia between MMTV-PyMT-, MMTV-PyMT+ and MMTV-PyMT+ without tumors ^{**} $P < 0.001$. GEE with normal distribution and identity link function using AR(1) correlation matrix between weeks followed by Bonferroni's multiple comparison. Values are expressed as means and SD.



Weeks	0	2	4	6	8	10	12
SED n = 9	9	9	9	8	5	5	3
TRA n = 12	12	12	12	12	12	8	8

Figure S2. Body weight in exercise-trained (TRA) and sedentary MMTV-PyMT+ mice (SED). Numbers in the table means number of mice throughout the weeks. GEE with normal distribution and identity link function using AR(1) correlation matrix between weeks. Values are expressed as means and SD.



Months	0	1	2	3
SED n = 9	9	9	8	5
TRA n = 12	12	12	12	11

Figure S3. Running distance in the exercise tolerance test in sedentary and exercise-trained groups. Numbers in the table mean number of mice throughout the months. GEE with normal distribution and identity link function using AR(1) correlation matrix between weeks. Values are expressed as means and SD. Reduction in the distance covered in the exercise tolerance tests performed during the experimental protocol (p-group=0.263, p-time<0.001 and p-interaction=0.069).

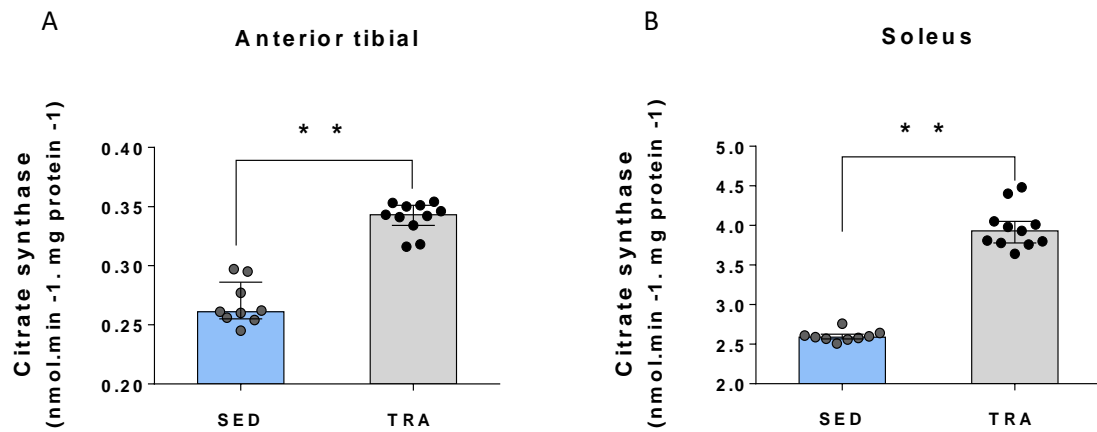


Figure S4. Measurement of the citrate synthase enzyme activity in the anterior tibial (A) and soleus muscle (B) in sedentary and trained MMTV-PyMT⁺. SED=Sedentary; TRA=Exercise-trained. ^{} $P < 0.001$, between group difference. Mann-Whitney's test. Values are expressed as medians and interquartile ranges (IQR). Animals/group: 9 SED and 11 TRA.**

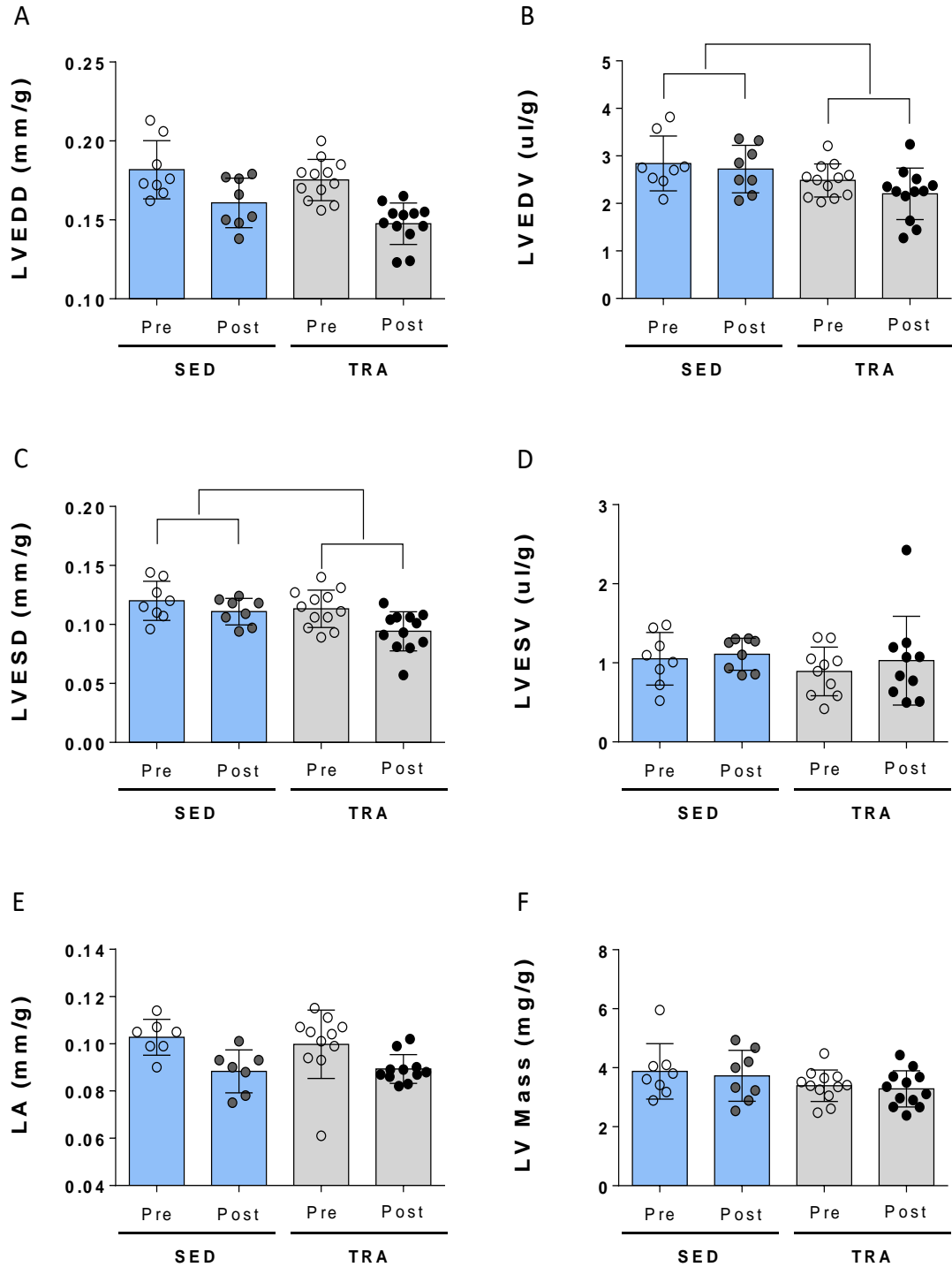


Figure S5. Morphological cardiac parameter in sedentary and exercise-trained MMTV-PyMT⁺ mice in the pre and post experimental protocol. A, Left ventricle end diastolic diameter (LVEDD); B, Left ventricle end diastolic volume (LVEDV); C, Left ventricle end systolic diameter (LVESD); D, Left ventricle end systolic volume (LVESV); E, Left atrium

(LA); F, Left ventricle mass (LV Mass). LVESD (p-group=0.038, p-interaction=0.226) and LVEDV (p-group=0.026, p-interaction=0.431) SED=Sedentary; TRA=Exercise-trained. GEE with normal distribution and identity link function using AR(1) correlation matrix between weeks. Values are expressed as means and SD. Animals/group: 8 SED and 12 TRA MMTV-PyMT+ mice. Two measures of LVESV in the exercise-trained MMTV-PyMT mice, and one measure of LA in each group were not obtained.

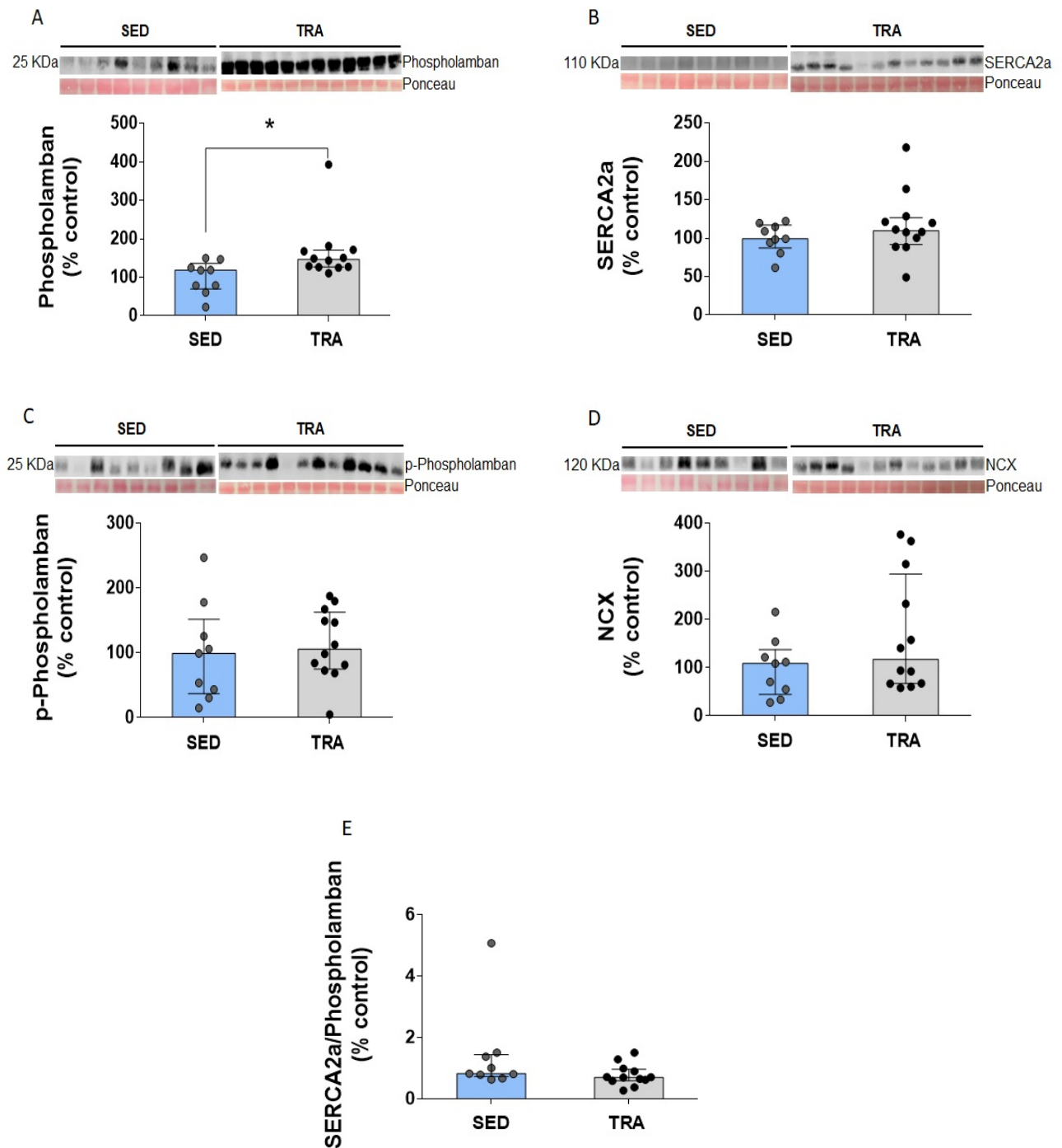


Figure S6. Cardiac myocyte calcium handling proteins in sedentary and exercise-trained MMTV-PyMT+ mice – A, Phospholamban; B, SERCA2a; C, phosphorilated phospholamban (p-phospholamban); D, sodium/calcium exchanger (NCX) and E, SERCA2a/phospholamban ratio. Western blot bands are shown for each figure. Exercise training did not improve phospholamban ($p=0.006$) and did not change SERCA2a ($p=0.345$), p-phospholamban

($p=0.554$), NCX ($p=0.247$) and SERCA2a/phospholamban ($p=0.111$). * $P<0.05$, between group difference. Animals/group: 9 sedentary (SED) and 12 exercise-trained (TRA). Mann-Whitney's test. Values are expressed as medians and interquartile ranges (IQR).